

Low-amplitude coherently coupled spatial soliton pairs due to both the linear and quadratic electro-optic effects

Hao Lili¹, Wang Qiang¹, Tang Hongxia², Mu Haiwei¹, Zhao Yuan³

(1. Department of Physics, Northeast Petroleum University, Daqing 163318, China;

2. College of Electrical Engineering, Suihua University, Suihua 152000, China;

3. Department of Physics, Harbin Institute of Technology, Harbin 150001, China)

Abstract: A comprehensive study of coherent coupling of low-amplitude spatial solitons that co-propagate in biased photorefractive crystals with both the linear and quadratic electro-optic effects was presented. Our results were shown that coherently coupled bright-bright and dark-dark spatial soliton pairs in the low-amplitude regime could be formed under appropriate conditions. The evolution equations, analytic solutions and the expressions of soliton pair widths of these low-amplitude coherently coupled spatial soliton pairs were obtained. It was proven that the existence, property and propagation of these soliton pairs due to co-effects of both the linear and quadratic electro-optic effects was greatly influenced by the photorefractive effects which could be enhanced, weakened or even counteracted because of the interaction of these two electro-optic effects. Moreover, the effects of three physical factors, i.e., the initial phase difference between two incident coherent beams, the intensity ratio and various external bias field on the existence conditions, properties of these low-amplitude coherently coupled soliton pairs have been discussed in detail. Finally, the self-deflection of low-amplitude bright-bright soliton pairs had also been investigated by means of perturbation procedure.

Key words: nonlinear optics; photorefractive spatial soliton; coherent coupling; electro-optic effect

CLC number: O437 **Document code:** A **DOI:** 10.3788/IRLA201948.S106006

线性和二次电光效应下小振幅相干耦合空间孤子对

郝丽丽¹, 王强¹, 唐红霞², 牟海维¹, 赵远³

(1. 东北石油大学物理系, 黑龙江大庆 163318; 2. 绥化学院电气工程学院, 黑龙江绥化 152000;

3. 哈尔滨工业大学物理系, 黑龙江哈尔滨 150001)

摘要: 研究了线性和二次电光效应共存的单光子光折变介质中小振幅情况下两个沿同一直线传播的空间光孤子间的相干耦合现象。研究结果表明在适当的条件下可以形成相干耦合暗-暗、亮-亮孤子对, 得到了相干耦合孤子对的光场方程、解析解和孤子对宽度的表达式。线性和二次电光效应间的

收稿日期: 2018-11-01; 修订日期: 2018-12-14

基金项目: 国家自然科学基金(51374072, 51774092, 41472126); 东北石油大学引导性创新基金(2018YDL-11);

东北石油大学国家自然科学基金培养基金(2017PYYL-07); 黑龙江省教育厅项目(12531838)

作者简介: 郝丽丽(1981-), 女, 博士生, 主要从事非线性光学和量子光学等方面的研究。Email: haolili0820@126.com

导师简介: 赵远(1963-), 男, 教授, 博士生导师, 主要从事激光雷达和光电信号检测等方面的研究。Email: zhaoyuan@hit.edu.cn

通讯作者: 王强(1980-), 男, 博士生, 主要从事量子干涉、度量和传感方面研究。Email: wangqiang8035@163.com

相互作用而产生相互增强、减弱甚至抵消的光折变效应对这些孤子对的形成、性质和传输规律具有重要的影响。另外,就两相干入射光的初始相位差、强度比和外加电场等三个因素对小振幅相干耦合孤子对的产生条件和性质的影响进行了详细的讨论。最后,采用微扰法分析了小振幅情况下亮-亮孤子对的自偏转效应。

关键词: 非线性光学; 光折变空间光孤子; 相干耦合; 电光效应

0 Introduction

In recent two decades, photorefractive (PR) spatial solitons have been extensively investigated because of their unique features of formation at low laser power (typically of the order of a few mW) and important potential applications for all-optical switching and routing, and so on^[1]. Besides the formation and properties of PR spatial solitons, the interactions between spatial solitons have also been at the front of current research. Amongst soliton interactions, soliton pairing is always a quite appealing issue. Research have shown that two incident beam will trap mutually in the PR materials under the influence of the nonlinear refractive-index modulation and then each of them propagates undistorted, i.e., coupled spatial soliton pairs form. Note, every component of coupled spatial soliton pairs depends on each other and each beam alone cannot survive as a soliton if the other beam is absent. In 1996, Christodoulides et al. firstly predicted incoherently coupled screening spatial soliton pairs^[2] and Chen et al. observed these soliton pairs experimentally^[3-4]. Soon later, Hou et al. presented that incoherently coupled multiple bright, dark and dark-bright hybrid screening-photovoltaic soliton families can be supported in biased photovoltaic PR materials^[5-6]. In addition, the interactions between other types of PR spatial solitons resulting only from the linear or quadratic electro-optic (EO) effect have also been widely studied^[7-8]. In recent years, spatial solitons and incoherently coupled soliton families (or soliton pairs) can exist in biased PR crystals involving both the linear and quadratic EO effects in steady-state regime^[9-15].

Given the above, the incoherent interaction of spatial solitons has already been widely concerned, whereas researches regarding the coherent interaction are relatively few. Even in the research field of coherent interactions, much attention has been paid to the coherent coupling of beams that propagate non-collinearly in PR materials, and most works are based on the experimental methods. In this paper, we investigate theoretically the existence and properties of the low-amplitude coherently coupled soliton pairs which propagate collinearly in biased PR crystals with both the linear and quadratic electro-optic effects. Moreover, the effects of the intensity ratio, the initial phase difference between two coherent incident beams and various external bias field on the existence conditions and characteristics of these coherently coupled soliton pairs will be discussed in detail. At the last part, the self-deflection of low-amplitude bright-bright soliton pairs will be analyzed by using perturbation procedure.

1 Theoretical model

We consider two mutually coherent low-amplitude incident beams that propagate collinearly along the axis in biased PR crystal with both the linear and quadratic EO effects which is put with its principal axes aligned with the x , y and z directions of the system. The polarization of coherent incident beams and an external bias electric field are both assumed to be parallel to the x -axis. For simplify, only the x -axis diffraction is taken into account. The optical fields of two low-amplitude coherent incident beams are expressed as the slowly varying envelopes, i.e., $\vec{E}_m(x,z) = \hat{x} \varphi_m(x,z) \exp[i(kz + \phi_m)]$ ($m=1,2$), ϕ_m represent

the initial phases of two coherent incident beams, $k = k_0 n_e = (2\pi/\lambda_0)n_e$ with n_e being the unperturbed index of refraction and λ_0 the free-space wavelength. Under these conditions, the two coherent beams satisfy the following equations^[1]:

$$\left(i \frac{\partial}{\partial z} + \frac{1}{2k} \cdot \frac{\partial^2}{\partial z^2} + \frac{k}{n_e} \Delta n \right) \varphi_m(x, z) = 0, \quad m=1, 2 \quad (1)$$

where the change of nonlinear refractive index Δn is governed by

$$\Delta n = -\frac{n_e^3 r_{33} E_{sc}}{2} - \frac{n_e^3 g_{\text{eff}} \varepsilon_0 (\varepsilon_r - 1)^2 E_{sc}^2}{2} \quad (2)$$

where r_{33} and g_{eff} are linear and the effective quadratic EO coefficients of PR crystal, respectively. ε_0 and ε_r are the vacuum and relative dielectric constants, respectively. E_{sc} is the space-charge field in the material. Under a strong bias field condition, the drift effect will be dominant, thus E_{sc} can be approximately expressed as^[16]:

$$E_{sc} = E_0 \frac{I_s + I_b + I_d}{I + I_b + I_d} - \frac{k_B T}{e} \frac{\partial I / \partial x}{I + I_b + I_d} \quad (3)$$

where I_b is the intensity of dark irradiance which is defined as $I_d = \beta/s$ with β being the dark generation rate and s the photoionization cross section of the photorefractive crystals. I_b is the intensity of the background beam, and if the background beam is not taken into account, its value is zero. $I = I(x, z) = (n_e/2\eta_0) \cdot \left(\sum_{k=m}^2 \varphi_m \right)^2$ is the total intensity of two incident beams with $\eta_0 = (\mu_0/\varepsilon_0)^{1/2}$. $E_0 = E_{sc}(x \rightarrow \pm\infty, z)$ and $I_s = I(x \rightarrow \pm\infty, z)$ represent the space charge field and the total intensity for $x \rightarrow \pm\infty$, respectively. In most cases, E_0 is approximately equal to $\pm V/W$, where V is the applied external voltage and W is the x -width of the PR crystal.

The normalized evolution equations can now be obtained by submitting Eqs.(2) and (3) into (1). For convenience, we adopt the following dimensionless parameters: $\xi = z/kx_0^2$, $s = x/x_0$, $\varphi_m = [2\eta_0(I_b + I_d)/n_e]^{1/2} U_m$ ($m = 1, 2$). x_0 is an arbitrary spatial width. Under these conditions, the envelopes U_m are found to obey

$$\begin{aligned} & i \frac{\partial U_m}{\partial \xi} + \frac{1}{2} \frac{\partial^2 U_m}{\partial s^2} - \frac{\beta_1(1+\rho)}{1 + \left| \sum_{m=1}^2 U_m \right|^2} U_m + \\ & \gamma_1 \frac{\left(\left| \sum_{m=1}^2 U_m \right|^2 \right)_s}{1 + \left| \sum_{m=1}^2 U_m \right|^2} U_m - \frac{\beta_2(1+\rho)^2}{\left(1 + \left| \sum_{m=1}^2 U_m \right|^2 \right)^2} U_m + \\ & \gamma_2 \frac{\left(\left| \sum_{m=1}^2 U_m \right|^2 \right)_s}{\left(1 + \left| \sum_{m=1}^2 U_m \right|^2 \right)^2} U_m - \\ & \gamma_3 \frac{\left[\left(\left| \sum_{m=1}^2 U_m \right|^2 \right)_s \right]^2}{\left(1 + \left| \sum_{m=1}^2 U_m \right|^2 \right)^2} U_m = 0, \quad m=1, 2 \quad (4) \end{aligned}$$

where, $\beta_1 = (k_0 x_0)^2 n_e^4 r_{33} E_0 / 2$, $\gamma_1 = k_0^2 x_0 n_e^4 r_{33} k_B T / 2e$, $\beta_2 = (k_0 x_0)^2 n_e^4 g_{\text{eff}} \varepsilon_0 (\varepsilon_r - 1)^2 E_0^2 / 2$, $\rho = I_s / (I_d + I_b)$, $\gamma_2 = k_0^2 x_0 n_e^4 g_{\text{eff}} \varepsilon_0 \cdot (\varepsilon_r - 1)^2 (k_B T) E_0 / e$, $\gamma_3 = k_0^2 n_e^4 g_{\text{eff}} \varepsilon_0 \times (\varepsilon_r - 1)^2 (k_B T)^2 / 2e^2$.

For simplicity, any loss effects have been neglected in our analysis. Note, the higher-order diffusion term of the PR γ_3 is quite small and will be omitted in the our analysis for $E_0 > 10^4$ V/m.

In the case of the low-amplitude case (i.e., $\rho \ll 1$ or $\left| \sum_{m=1}^2 U_m \right|^2 \ll 1$), Eq.(4) is equivalent to

$$\begin{aligned} & i \frac{\partial U_m}{\partial \xi} + \frac{1}{2} \frac{\partial^2 U_m}{\partial s^2} - \beta_1(1+\rho) \left(1 - \left| \sum_{m=1}^2 U_m \right|^2 \right) U_m + \\ & \gamma_1 \left(1 - \left| \sum_{m=1}^2 U_m \right|^2 \right) \left(\left| \sum_{m=1}^2 U_m \right|^2 \right)_s U_m - \\ & \beta_2(1+\rho)^2 \left(1 - 2 \left| \sum_{m=1}^2 U_m \right|^2 \right) U_m + \\ & \gamma_2 \left(1 - 2 \left| \sum_{m=1}^2 U_m \right|^2 \right) \left(\left| \sum_{m=1}^2 U_m \right|^2 \right)_s U_m = 0 \quad (5) \end{aligned}$$

Under strong bias conditions, the diffusion effect can be neglected, i.e., $\gamma_1 = \gamma_2 = 0$, then Eq. (5) is reduced to

$$i \frac{\partial U_m}{\partial \xi} + \frac{1}{2} \frac{\partial^2 U_m}{\partial s^2} - \beta_1(1+\rho) \left(1 - \left| \sum_{m=1}^2 U_m \right|^2 \right) U_m - \beta_2(1+\rho)^2 \left(1 - 2 \left| \sum_{m=1}^2 U_m \right|^2 \right) U_m = 0 \quad (6)$$

which is a modified nonlinear schrödinger equation (NLSE) and can be solved analytically.

2 Results and discussions

In what follows, we will present low-amplitude coherently coupled bright-bright and dark-dark soliton pair solutions in the steady-state regime. The existence conditions and properties of these soliton pair will be discussed in detail.

2.1 Low-amplitude coherently coupled bright-bright soliton pair

For bright-bright soliton pair, $I(0)=I_{max}$, $\rho=I_c/(I_b+I_d)=0$ and then the Eq.(6) can be reduced to

$$i \frac{\partial U_m}{\partial \xi} + \frac{1}{2} \frac{\partial^2 U_m}{\partial s^2} - \beta_1 \left(1 - \left| \sum_{m=1}^2 U_m \right|^2 \right) U_m - \beta_2 \left(1 - 2 \left| \sum_{m=1}^2 U_m \right|^2 \right) U_m = 0, \quad m=1,2 \quad (7)$$

To obtain the low-amplitude coherently coupled bright-bright soliton pair solution, we assume $U_m(s, \xi) = r_m^{1/2} y(s) \exp[i(v\xi + \phi_m)]$ ($m=1,2$) where v represents a nonlinear shift of the propagation constant, ϕ_m denotes the initial phase of two coherent beams. r_m are defined as $r_m = I_{max}/(I_b + I_d) = I_m(0)/(I_b + I_d)$. $y(s)$ is a normalized real function and satisfies $y(0)=1$, $y'(0)=0$, $y(s \rightarrow \pm\infty) = 0$ and all the derivatives of $y(s)$ are zeros when $s \rightarrow \pm\infty$. Substituting the expressions U_m into Eq.(7), we get

$$U_m(s, \xi) = r_m^{1/2} \operatorname{sech} \{ [(\beta_1 + 2\beta_2)r]^{1/2} s \} \times \exp \{ i \{ [(r/2 - 1)\beta_1 + (r - 1)\beta_2] \xi + \phi_m \} \} \quad (8)$$

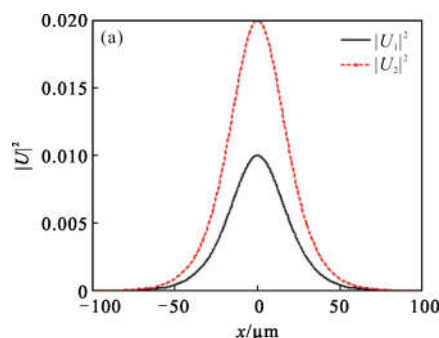
where $r = r_1 + r_2 + 2(r_1 r_2)^{1/2} \cos \Delta\phi$ with $\Delta\phi = \phi_1 - \phi_2$ being the phase difference between two coherent incident beams. By Eq.(8), it is easy to see that the existence condition of the bright-bright soliton pair is $\beta_1 + 2\beta_2 > 0$. Moreover, the intensity FWHM can be obtained directly

$$\Delta x_b = \frac{2\sqrt{2} \ln(\sqrt{2} + 1)}{k_0 n_e^4 \{ [r_{33} E_0 + 2g_{\text{eff}} \epsilon_0 (\epsilon_r - 1)^2 E_0^2] r \}^{1/2}} \quad (9)$$

Quite different from the cases investigated previously, the low-amplitude bright-bright soliton pair in our analysis can also exist when $\beta_1 \beta_2 < 0$ so long as $\beta_1 + 2\beta_2 > 0$ is satisfied. Further, the two components of soliton pair can also be obtained by $U_m(s, \xi) = r_m^{1/2} y(s) \exp[i(v\xi + \phi_m)]$, $m=1,2$.

To illustrate our results, we take PMN-0.33PT single crystal which shows maximal transparency, very good optical clarity and low propagation loss for example. The parameters of PMN-PT are $g = g_{\text{eff}} \epsilon_0 (\epsilon_r - 1)^2 = 1.36 \times 10^{-16} \text{ m}^2/\text{V}^2$, $n_e = 2.562$, $r_{33} = 40 \times 10^{-12} \text{ m/V}^{[17-21]}$. Other parameters are adopted as $\lambda_0 = 632.8 \text{ nm}$, $x_0 = 40 \text{ }\mu\text{m}$, $r_1 = 0.01$.

Figure 1 depicts the intensity profiles of soliton components of low-amplitude coherently coupled bright-bright soliton pair components for Fig.1(a) $\Delta\phi = \pi/4$ and Fig.1(b) $\Delta\phi = \pi/2$ when $r_2/r_1 = 2$, $E_0 = 2 \times 10^5 \text{ m/V}$. Based on the above parameters, we get $\beta_1 = 27.18$ and $\beta_2 = 18.53$. The FWHMs of bright-bright soliton pair are $39.34 \text{ }\mu\text{m}$ and $50.79 \text{ }\mu\text{m}$, respectively. Obviously, the phase difference $\Delta\phi$ has an impact on the widths of soliton pair. Besides $\Delta\phi$, for coherently coupled soliton pair which propagates collinearly, the soliton pair width Δx is also closely connected with both the intensity ratio of two coherent beams r_2/r_1 and external electric field E_0 . Figure 2 shows the dependence of Δx on $\Delta\phi$ with different r_2/r_1 in the case of the same E_0 , and Figure 3 depicts the widths Δx versus $\Delta\phi$ with the same r_2/r_1 under different E_0 conditions.



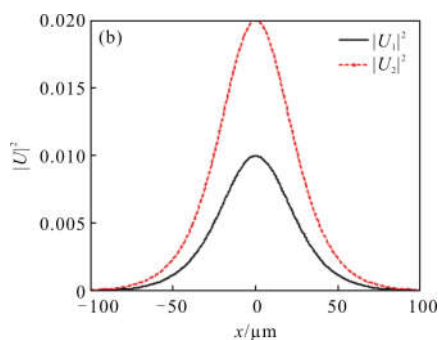


Fig.1 Intensity profiles of soliton components of the low-amplitude coherently coupled bright- bright soliton pair for (a) $\Delta\phi=\pi/4$ and (b) $\Delta\phi=\pi/2$ when $r_2/r_1=2$, $E_0=2\times 10^5$ m/V

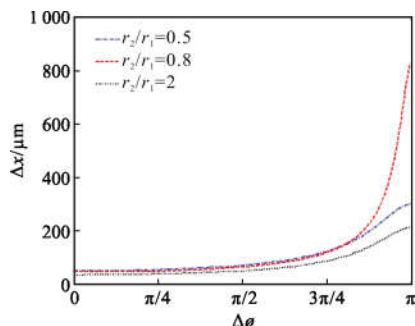


Fig.2 Curve of the low-amplitude coherently coupled bright-bright soliton pair width Δx versus $\Delta\phi$ under different r_2/r_1 conditions for $E_0=2\times 10^5$ m/V

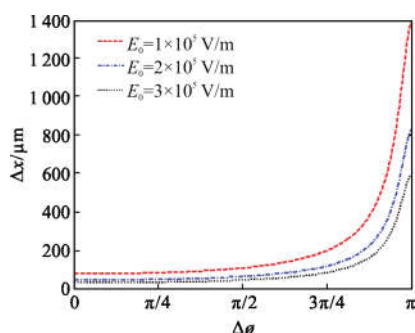


Fig.3 Width Δx of low-amplitude coherently coupled bright-bright soliton pair versus $\Delta\phi$ under different E_0 conditions for $r_2/r_1=0.8$

From above two figures, it is evident that the width always increases as $\Delta\phi$ rises, the reason for this kind of trend appeared is that the value of decreases monotonically with ascending of $\Delta\phi$ in the range of $0-\pi$ which can be obtained easily by $r=r_1+r_2+2(r_1r_2)^{1/2}\cos\Delta\phi$, so in the low-amplitude region Δx will always increase when r goes down. Moreover, Δx

decreases with ascending of r and E_0 when $\Delta\phi$ is kept constant. Figure 4 illustrates the dependence of Δx on r_2/r_1 for $E_0=2\times 10^5$ V/m under different $\Delta\phi$ conditions, from which we can see that when $\Delta\phi$ is far away from π the width Δx is slightly affected when r_2/r_1 rises. However, when $\Delta\phi$ is close to π or even $\Delta\phi=\pi$, the dependence of Δx on r_2/r_1 rapidly goes down when r_2/r_1 goes up. Obviously, the results shown in Fig.4 are consistent with that of Fig.2.

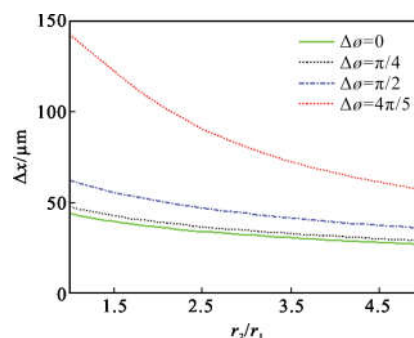


Fig.4 Width Δx of bright-bright soliton pair versus r_2/r_1 for $E_0=2\times 10^5$ m/V

2.2 Low-amplitude coherently coupled dark-dark soliton pair

The case of dark-dark soliton pairs can be analyzed in a similar fashion, except I_∞ and ρ are finite quantities now. Let $U_m(s, \xi) = \rho_m^{1/2} y(s) \exp[i(\nu\xi + \phi_m)]$, $m=1,2$ with $\rho_m = I_{m\max}/(I_b + I_d) = I_{m\infty}/(I_b + I_d)$. Here the parameters ν , ϕ_m are the same as the bright-bright soliton pair. $y(s)$ is a normalized odd function bounded between $0 \leq |y(s)| \leq 1$, i.e., $y(0)=0$, $y(s \rightarrow \pm\infty) = \pm 1$, and all the derivatives of $y(s)$ are zeros when $s \rightarrow \pm\infty$. Substitution of the latter U_m into Eq.(6) yields

$$U_m(s, \xi) = \rho_m^{1/2} \tanh\{ \{-[\beta_1(1+\rho) + 2\beta_2(1+\rho)^2]\rho\}^{1/2} s \} \cdot$$

$$\exp\{i\{[-\beta_1(1-\rho^2) + \beta_2(1+\rho)^2(2\rho-1)]\xi + \phi_m\}\} \quad (10)$$

where $\rho = \rho_1 + \rho_2 + 2(\rho_1\rho_2)^{1/2}\cos(\phi_1 - \phi_2)$. Obviously, the existence condition for dark-dark soliton pair in the low-amplitude case is $\beta_1 + 2\beta_2(1+\rho) < 0$. The intensity FWHM can be directly given by

$$\Delta x_d = \frac{2\sqrt{2} \ln(\sqrt{2} + 1)}{k_0 n_e^4 \{ [r_{33}(1+\rho)E_0 + 2g_{\text{eff}}\epsilon_0^2 \times (\epsilon_r - 1)^2(1+\rho)^2 E_0^2] \rho \}^{1/2}} \quad (11)$$

Similarly, the signs of β_1 and β_2 can be different

as long as $\beta_1 < -2\beta_2$ which also is different from the previous cases (where $\beta_1 < 0$ is the necessary condition for dark solitons due to linear EO effect or $\beta_2 < 0$ for quadratic EO effect). Then soliton components of dark-dark soliton pairs can be obtained by $U_m(s, \xi) = \rho_m^{1/2} y(s) \cdot \exp[i(\nu\xi + \phi_m)]$, $m=1,2$.

Figure 5 illustrates the intensity profiles of the low-amplitude dark-dark soliton pairs for Fig.5 (a) $\Delta\phi=0$, and Fig.5(b) $\Delta\phi=\pi/2$ when $\rho_2/\rho_1=1.5$ and $E_0 = -1 \times 10^5$ V/m. The FWHMs are $115.73 \mu\text{m}$ and $156.51 \mu\text{m}$, respectively. Figure 6 shows the dependence of Δx on $\Delta\phi$ for $\rho_2/\rho_1=0.6, 1.6, 2.4$ and $E_0 = -1 \times 10^5$ V/m, from which we can see that Δx increases slowly when $\Delta\phi$ is small and then increases rapidly when $\Delta\phi \rightarrow \pi$. But beyond that, Δx always decreases with ρ_2/ρ_1 , whether $\Delta\phi$ is far away from π , close to π or even $\Delta\phi = \pi$. Besides, when $\Delta\phi$ approaches to π the value of ρ will be lower if $\rho_2/\rho_1 \rightarrow 1$, so in this case Δx is very large, as shown in Fig.7.

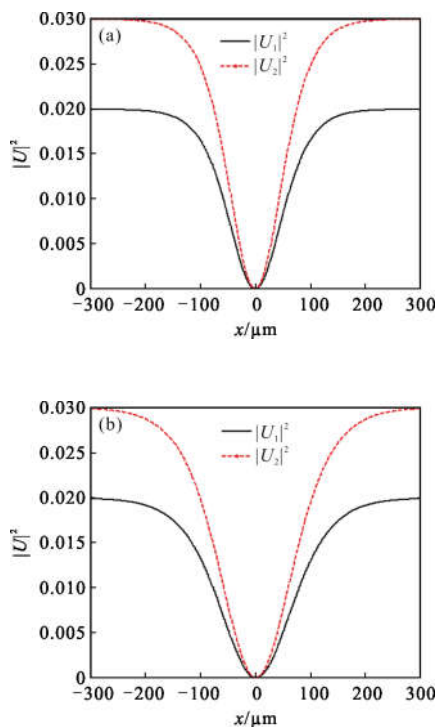


Fig.5 Intensity profiles of soliton components of the dark-dark soliton pair for (a) $\Delta\phi=0$ and (b) $\Delta\phi=\pi/2$ when $\rho_2/\rho_1=1.5$ and $E_0 = -1 \times 10^5$ V/m

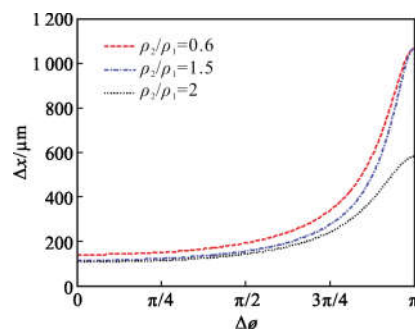


Fig.6 Width Δx of the low-amplitude coherently coupled dark-dark soliton pair versus the initial phase difference $\Delta\phi$ for $E_0 = -1 \times 10^5$ V/m with ρ_2/ρ_1 chosen as 0.6, 1.5 and 2

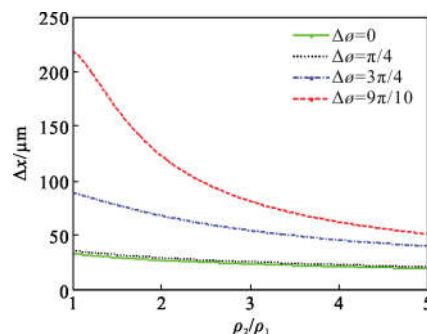


Fig.7 Width Δx of coherent coupled dark-dark soliton pair versus the intensity ratio ρ_2/ρ_1 for $E_0 = -1 \times 10^5$ V/m with different four $\Delta\phi$

2.3 Self-deflection of the low-amplitude coherently coupled bright-bright soliton pair

The self-deflection effect can be systematically studied by using perturbation procedure. Since the evolution of soliton beam under the action of diffusion process is approximately adiabatic, we make the following ansatz:

$$U_m(s, \xi) = r_m^{1/2} y[s+q(\xi)] \times \exp\{i[\nu\xi + \omega(\xi)[s+q(\xi)] + \sigma(\xi) + \phi_m]\} \quad (12)$$

where $U_m(s, \xi) = r_m^{1/2} y(s) \exp[i(\nu\xi + \phi_m)]$ is the steady-state low-amplitude bright-bright soliton pair solution when $\gamma_1 = \gamma_2 = 0$, and $q(\xi)$ represents a lateral shift in the position of the beam center, $\omega(\xi)$ is associated with the angle between the central wave-vector of the beam and the propagation ξ axis, and $\sigma(\xi)$ is a phase factor permitted to vary during propagation. After a straightforward calculation, we arrive at

$$\begin{aligned} K_1(r) &= K_1'(r) = -2r^2/15 \\ K_2(r) &= K_2'(r) = -4r^2/15 \end{aligned} \quad (13)$$

Then $\omega(\xi)$, $q(\xi)$, $\sigma(\xi)$ can be expressed as

$$\begin{aligned} \omega(\xi) &= -8(\gamma_1 + \gamma_2)(\beta_1 + 2\beta_2)r^2\xi/15 \\ q(\xi) &= 4(\gamma_1 + \gamma_2)(\beta_1 + 2\beta_2)r^2\xi^2/15 \\ \sigma(\xi) &= 8[2(\gamma_1 + \gamma_2)(\beta_1 + 2\beta_2)r^2/15]^2\xi^3/3 \end{aligned} \quad (14)$$

The lateral and angular deflection x_d and θ_d in the low-amplitude region can then be obtained from

$$\begin{aligned} x_d &= -\frac{4}{15}r^2\{(k_0r_{33}n_e^3)^2(k_B T/4e)E_0 + (kn_e^3)^2 \cdot \\ & r_{33}g_{\text{eff}}\varepsilon_0^2(\varepsilon_r - 1)^2(k_B T/4e)E_0^3 + [kn_e^3g_{\text{eff}}\varepsilon_0^2(\varepsilon_r - 1)^2]^2 \cdot \\ & (k_B T/4e)E_0^3\}z^2 \end{aligned} \quad (15)$$

$$\begin{aligned} \theta_d &= -\frac{8}{15}r^2\{(k_0r_{33}n_e^3)^2(k_B T/4e)E_0 + (kn_e^3)^2 \cdot \\ & r_{33}g_{\text{eff}}\varepsilon_0^2(\varepsilon_r - 1)^2(k_B T/4e)E_0^2 + [kn_e^3g_{\text{eff}}\varepsilon_0^2(\varepsilon_r - 1)^2]^2 \cdot \\ & (k_B T/4e)E_0^3\}z \end{aligned} \quad (16)$$

From Eqs.(14) and (15), it is easy to obtain that the center of soliton pairs follows a parabolic trajectory, whereas the central spatial frequency component shifts linearly with the propagation distance.

In Fig.8, we provide the curve of spatial shift x_d for the low-amplitude bright-bright soliton pairs with different r_2/r_1 when $E_0=1 \times 10^5$ V/m, from which we can see that x_d increases with the increase of r_2/r_1 in the low-amplitude region. Figure 9 depicts the dependence of x_d on $\Delta\phi$ at different three values of 0, $\pi/4$, $\pi/2$, it is easy to see that x_d decreases as $\Delta\phi$ rises. The explanation of this could be that $|K(r)|$ increases as r increases and decreases as r decreases.

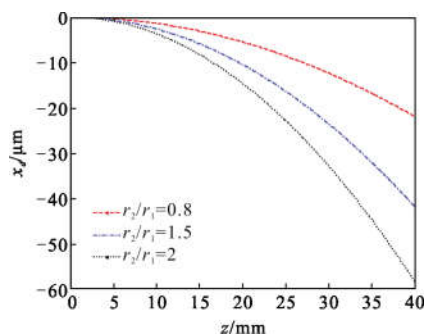


Fig.8 Evolution of the spatial shift x_d obtained from the perturbation procedure for the low-amplitude bright-bright soliton pairs when $E_0=1 \times 10^5$ V/m, $\Delta\phi=\pi/4$ with different value of r_2/r_1

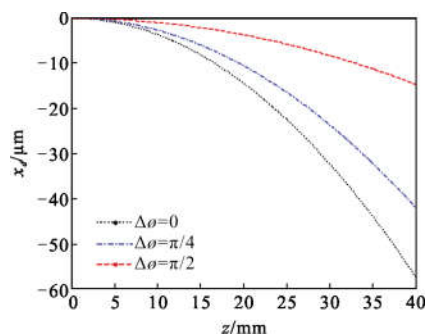


Fig.9 Evolution of the spatial shift x_d obtained from the perturbation procedure for the low-amplitude bright-bright soliton pairs when $E_0=1 \times 10^5$ V/m, $r_2/r_1=1.5$ and $\Delta\phi=0, \pi/4, \pi/2$

3 Conclusions

In conclusion, the existence of the low-amplitude coherently coupled bright-bright and dark-dark spatial soliton pairs propagating collinearly in biased PR crystal with both the linear and quadratic EO effects are proved theoretically. It is found that these soliton pairs owe their existence to both the linear and quadratic EO effects in the meantime. The evolution equations, existence conditions, analytic solutions and properties of these soliton pairs have been discussed in detail. It is found that the intensity ratio r_2/r_1 (or ρ_2/ρ_1), the phase difference $\Delta\phi$ between two incident low-amplitude coherent beams and various electric fields have a major influence on the soliton pair widths Δx . Our results show that the widths Δx_b (or Δx_d) of bright-bright (or dark-dark) soliton pairs in the low-amplitude region increases slowly as $\Delta\phi$ rises when the value of $\Delta\phi$ is not too close to π . Moreover, Δx_b (or Δx_d) always decreases when the intensity ratio r_2/r_1 (or ρ_2/ρ_1) and E_0 goes up. However, if r_2/r_1 (or ρ_2/ρ_1) approaches to 1, Δx_b (or Δx_d) increases rapidly with increasing of $\Delta\phi$ when $\Delta\phi \rightarrow \pi$ or even $\Delta\phi = \pi$. Finally, the self-deflection of bright-bright soliton pairs have been investigated by exploiting the perturbation procedure. It is shown that the center of soliton pair follows a parabolic trajectory, whereas the central spatial frequency component shifts linearly with the propagation distance. The spatial shift x_d of the low-amplitude bright-bright soliton pairs increases with

the increase of r_2/r_1 and decreases as $\Delta\phi$ rises.

References:

- [1] Chen Z, Segev M, Christodoulides D N. Optical spatial solitons: historical overview and recent advances [J]. *Reports on Progress in Physics*, 2012, 75(8): 086401.
- [2] Christodoulides D N, Singh S R, Carvalho M I, et al. Incoherently coupled soliton pairs in biased photorefractive crystals [J]. *Applied Physics Letters*, 1996, 68 (13): 1763–1765.
- [3] Chen Z, Segev M, Coskun T H, et al. Observation of incoherently coupled photorefractive spatial soliton pairs [J]. *Optics Letters*, 1996, 21(18):1436–1443.
- [4] Chen Z, Segev M, Coskun T H, et al. Incoherently coupled dark-bright photorefractive solitons [J]. *Optics Letters*, 1996, 21(22): 1821–1823.
- [5] Hou C, Zhou Z, Yuan B, et al. Incoherently coupled bright-dark hybrid soliton families in biased photovoltaic-photorefractive crystals [J]. *Applied Physics B (Lasers and Optics)*, 2001, 72(2): 191–194.
- [6] Hou C, Li B, Sun X. Incoherently coupled screening-photovoltaic soliton families in biased photovoltaic photorefractive crystals[J]. *Chin Phys*, 2001, 10(4): 310–313.
- [7] Su Y L, Jiang Q C, Ji X M. Electromagnetism, optics, acoustics, heat transfer, classical mechanics, and fluid dynamics:incoherently coupled grey-grey spatial soliton pairs in biased two-photon photovoltaic photorefractive crystals[J]. *Communications in Theoretical Physics*, 2010, 53(5): 943–946.
- [8] Jiang Q C, Liu J S. Incoherently coupled spatial soliton pairs in biased centrosymmetric photorefractive media with a resistance[J]. *Laser Technol*, 2011, 35(1): 70–73.
- [9] Hao L, Hou C, Wang Q. Incoherently coupled spatial soliton families in biased two-photon photorefractive crystals with both the linear and quadratic electro-optic effect [J]. *Chin Opt Lett*, 2014, 12(4): 041901.
- [10] Hao L, Wang Q, Hou C. Incoherently coupled spatial soliton pairs due to both the linear and quadratic electro-optic effects[J]. *Journal of Modern Optics*, 2015, 62(3): 205–211.
- [11] Jiang Q, Su Y, Nie H, et al. Separate spatial soliton pairs in a biased series photorefractive crystal circuit with both the linear and quadratic electro-optic effects [J]. *Journal of Modern Optics*, 2017, 64(6): 609–615.
- [12] Jiang Q, Su Y, Nie H, et al. New type gray spatial solitons in two-photon photorefractive media with both the linear and quadratic electro-optic effects [J]. *Journal of Nonlinear Optical Physics & Materials*, 2017, 26(1): 1750006.
- [13] Katti A, Yadav R A, Prasad A. Bright optical spatial solitons in photorefractive waveguides having both the linear and quadratic electro-optic effect[J]. *Wave Motion*, 2018, 77: 64.
- [14] Katti A. Incoherently coupled Gaussian soliton pairs in biased photorefractive crystal having both the linear and quadratic electro-optic effect[J]. *Applied Physics B*, 2018, 124(9): 192.
- [15] Hao Lili, Hou Chunfeng, Mu Haiwei, et al. Coherently coupled soliton pairs in biased two-photon photorefractive crystals with both linear and quadratic electro-optic effects [J]. *Infrared and Laser Engineering*, 2016, 45(S1): S108001. (in Chinese)
- [16] Christodoulides D N, Carvalho M I. Bright, dark, and gray spatial soliton states in photorefractive media [J]. *J Opt Soc Am B*, 1995, 12(9): 1628–1633.
- [17] Wan X, Wang D Y, Zhao X, et al. Electro-optic characterization of tetragonal $(1-x)\text{Pb}(\text{Mg}_{1/3}\text{Nb}_{2/3})\text{O}_3-x\text{PbTiO}_3$ single crystals by a modified s enarmont setup [J]. *Solid State Commun*, 2005, 134 (8): 547–551.
- [18] Kumar P, Sharma S, Thakur O P, et al. Dielectric, piezoelectric and pyroelectric properties of PMN–PT(68:32) system[J]. *Ceram Int*, 2004, 30(4): 585–589.
- [19] Zhang R, Jiang B, Cao W. Single-domain properties of $0.67\text{Pb}(\text{Mg}_{1/3}\text{Nb}_{2/3})\text{O}_3-0.33\text{PbTiO}_3$ single crystals under electric field bias[J]. *Appl Phys Lett*, 2003, 82(5): 787–789.
- [20] Wei Z, Huang Y, Tsuboi T, et al. Optical characteristics of Er^{3+} -doped PMN–PT transparent ceramics [J]. *Ceram Int*, 2012, 38(4): 3397–3402.
- [21] Colla E V, Yushin N K, Viehland D. Dielectric properties of $(\text{PMN})_{(1-x)}(\text{PT})_x$ single crystals for various electrical and thermal histories[J]. *J Appl Phys*, 1998, 83(6): 3298–3304.